Applied Thermal Engineering 104 (2016) 139–145

Contents lists available at ScienceDirect

Applied Thermal Engineering

journal homepage: www.elsevier.com/locate/apthermeng

Research Paper

Investigation of the flat disk-shaped LHP with a shared compensation chamber

Song He, ZhiChun Liu *, DongDong Wang, Jing Zhao, Wei Liu, JinGuo Yang

School of Energy and Power Engineering, HuaZhong University of Science and Technology, Wuhan 430074, China

HIGHLIGHTS

- A flat disk-shaped evaporator with a shared compensation chamber is put forward.
- The evaporator heat transfer capacity increases from 210 W for one heating surface to 240 W for two heating surfaces.
- The loop demonstrates a good response to alternative heat load applied to two heating surfaces.
- The co-evaporation of two primary wicks enhances the operating performance of the LHP.

GRAPHICAL ABSTRACT

One of the main advantages of the flat evaporator with a shared CC is that two heating surfaces can be used to dissipate heat. Aiming at the feature of the evaporator structure, two heating surfaces applied to alternative heat load is studied experimentally when the heat transfer capacity of the evaporator is fixed at 160 W. Fig. 1 gives the operating curve of the LHP with a fixed total heat load of 160 W, the black line represents the change of heat load to heating surface 2 and the red stands for heating surface 1. The LHP can make a fast response to variable heat load and operate stably, reflecting the good operating performance of the evaporator with a shared CC.

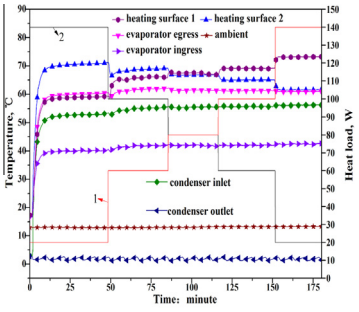

Fig. 1 Continuous operation with alternative heat load

ARTICLE INFO

Article history:
Received 16 February 2016
Revised 20 April 2016
Accepted 6 May 2016
Available online 10 May 2016

Keywords:
Loop heat pipe
Biporous wick
Two heating surfaces
Shared CC
Limited space

ABSTRACT

Conventional flat loop heat pipes only possess one active zone, not satisfying the requirements for the special occasions. In this paper, an evaporator with a shared compensation chamber is developed for cooling the compact electronic devices. Its main feature is the compensation chamber shared by two heating surfaces, the shared compensation chamber plays a role in supplying to two wicks when two heating surfaces are heated simultaneously. Under the conditions of the favorable elevation with a slope of 10° in the gravity field and the working fluid inventory with 75%, its startup performance and characteristics of operation with variable heat load have been studied. At two different heat sink temperatures of 0 °C and −5 °C, the loop could start up successfully at different heat load arrangements. With the evaporator wall temperature below (90 ± 2) °C, the transferred maximum heat load was 240 W. Especially, start-up process with two heating surfaces was improved, and the temperature difference between two heating surfaces was less than 1 °C. Otherwise, given the constant total heat load of 160 W, the system demonstrated very fast response to alternative heat load applied to two heating surfaces.

* Corresponding author at: 318 Power Building, 1037 Luoyu Road, Hongshan District, Wuhan 430074, China.
E-mail address: zcliu@hust.edu.cn (Z. Liu).

http://dx.doi.org/10.1016/j.applthermaleng.2016.05.043
1359-4311/

Nomenclature

T_{ej}	average temperature of heating surface j (j = 1, 2), (j = 1, Tc1, Tc2, Tc3, Tc5; j = 2, Tc20, Tc21, Tc22, Tc23), °C
$T_{e\text{-}out}$	evaporator egress temperature, (Tc6), °C
T_{cond}	average temperature of the condenser inlet and outlet, (Tc8, Tc9), °C
Q_j	heat load applied to heating surface j (j = 1, 2), W
Kei	heat transfer coefficient with heating surface 2 only (i = 0) or with heating surface j (i = 1, j = 1; i = 2, j = 2) for operation with equal heat load, W/(cm^2 K)
F_e	the heating area, cm^2
V_{total}	internal volume of the loop, ml
V_{cond}	condenser volume, ml
V_{CC}	CC volume, ml
V_{ll}	volume of the liquid volume, ml
W_{wick}	volume of porosity in the wick, ml
α	the ratio of the charging working fluid volume to the cavity volume of the loop
β	vapor phase share in the CC that is an experienced value

1. Introduction

Cooling technology for electronics with large power or high heat flux has been urgently in demand. Loop heat pipes (LHPs) are considered to be highly efficient heat-transfer device with a great potential for development and applications in the fields of thermal management, and are expected to address thermal control in terrestrial electronics [1,2]. Many scholars have made much effort to study the heat transfer performance of the LHPs experimentally and theoretically since the first LHP was invented in 1970s [3–7]. The main component of the LHP system is the evaporator. Among the existing LHP designs, the shape of the evaporator may be cylindrical or flat, which depends on the purpose, the shape and heat source dimensions, and the working fluid used [8]. Compared with cylindrical evaporators, flat evaporators have advantages of its flat thermal contact surface and high isothermality [9]. LHPs with flat evaporator (F-LHPs) attract extensive attention owing to its remarkable advantages above. Therefore, the operating characteristics of F-LHPs, including startup process, variable heat load operation, temperature fluctuations and thermal resistance, have been considerably investigated, providing guidance for its development and applications.

For the successful applications of the LHP systems to the compact electronic device cooling with high power density, the appropriate structure of the evaporator doesn't only improve the heat transfer capacity of LHPs, but also necessary for limited space. Singh et al. [10] proposed a mLHP with only 5 mm thickness of a flat evaporator for the cooling of high performance microprocessors for electronic devices, and achieved good performance. Xuan et al. [11] investigated a circular flat evaporator with an outer diameter of 41 mm and a thickness of 15 mm, specially designed for cooling electronic devices. Lin et al. [12] studied the dual compensation chamber loop heat pipe, revealing the unstable phenomena of the temperature fluctuations, temperature hysteresis and transient penetration of vapor. For reducing the influence of heat leak from the evaporator to the compensation chamber (CC), Wang et al. [13,14] proposed a LHP with two primary wicks inserted the evaporator.

The capillary force developing on the evaporator wick works as the driving force of the working fluid circulation. Thus, wick structures are regarded as an important factor in order to improve the operating performance of LHPs. The inner wick structures are changed from the monoporous to the biporous where the large pores play a role in reducing flow resistance and providing the extra evaporating area, making the performance of capillary wicks dramatically promoted [15–18]. In addition, multilayer wicks were investigated to obtain good heat conduction and reduce heat leakage in [19,20].

In order to apply the LHPs to the compact electronic devices and overcome the disadvantages of the cylindrical evaporators, Wukchul et al. [21,22] have ever proposed a flat bifacial evaporator loop heat pipe and investigated its operating characteristic. In the present study, a new evaporator structure with a shared CC is designed, fabricated and conducted. The shared CC is able to supply the working fluid for two wicks located in the evaporator simultaneously, liquid vaporization occurred on the two heating surfaces amounts to two flat evaporators for thermal management, saving the reserved space for the thermal control equipment and improving startup performance. Two surfaces of the evaporator can be used to dissipate heat, extending the function of the existing F-LHPs. Compared with the cylindrical evaporator absorbing heat from two heating surfaces, the evaporator with a shared CC reduces the mass and thermal resistance of the LHP system, and also can operate with one surface or two surfaces simultaneously. During the tests, two heat source simulators act as two different instruments, its startup performance and characteristics of operation with variable heat load cycle were analyzed at two different heat sink temperature of 0 °C and −5 °C, respectively.

2. Experimental setup

The test device is a methanol-copper LHP with two nickel wicks as the primary wick and a circular stainless wire mesh as the secondary wick. Table 1 summarizes the geometric parameters of the components, where O.D. and I.D. represent the outer and inner diameters, respectively. The whole experimental system consists of LHP system, heat source simulator, heat sink temperature control system, and data acquisition system. Fig. 1(a) presents the schematic diagram of the LHP system, including the evaporator, liquid and vapor transport lines, the tube-in-tube condenser. Fig. 1(b) gives details of the inner evaporator structure, the transport line connects the evaporator ingress and the evaporator

Table 1
The geometric parameters of the components.

Components	Dimensions	Value
The evaporator	O.D./height	43.30/16.65 (mm)
The nickel wick 1	Thickness/groove width/groove depth	4.26/2/1.59 (mm)
	Porosity	75%
The nickel wick 2	Thickness/groove width/groove depth	4.21/2/1.59 (mm)
	Porosity	78%
Circular stainless steel wire mesh	O.D./I.D./thickness	37.6/27/6 (mm)
Vapor line	O.D./I.D./length	4/3/330 (mm)
Liquid line	O.D./I.D./length	4/3/490 (mm)
Condenser	O.D. for the working fluid	4 (mm)
	O.D. for the coolant	12 (mm)
	Length	802 (mm)

egress, forming the closed loop. The condenser is linked to heat sink temperature control system, which can reach the lowest temperature of −15 °C and the minimal temperature control accuracy is 1 °C. The condensation section is long enough to guarantee that cold liquid exiting the condenser gains certain degree of subcooling. A copper cylinder with three embedded cartridge heater works as heat source simulator, the heater is directly controlled by the voltage regulator and the wattmeter, regulating and maintaining the applied heat load.

For the sake of reducing heat loss to the ambient, heat source simulator and the transport line are wrapped with 10 mm thickness adiabatic material with conductivity of 0.012 W/m K. All the components are connected to the keithley 2700 data acquisition system through the 24 T-type thermocouples, which helps to monitor and record the temperature signal from the LHP, the locations of the thermocouple are shown in Fig. 1(a). In order to minimize the impact of the non-condensable gas on operating temperature, the loop is evacuated to the pressure 4.1×10^{-4} Pa before charging the working fluid.

The CC plays a vital role in supplying liquid to wicks, whose size and location determine the operating performance of the LHP. The proper design of the CC can not only guarantee sufficient liquid to the wicks, but also reduce the thickness of the evaporator. Therefore, efforts are made to design the CC for meeting with two requirements above as far as possible. Two nickel wicks and a secondary wick encircle an annular cavity, working as the CC. The charge ratio can be determined based on the following equations:

$$\alpha V_{total} > V_{cond} + V_{ll} + V_{wick} + (1-\beta)V_{cc} \quad (1)$$

$$\alpha V_{total} < V_{cond} + V_{ll} + V_{wick} + V_{cc} \quad (2)$$

For this CC structure, we chose the value $\beta = 0.5$ and the value α ranged from 0.69 to 0.77. Finally, the value α is determined at 0.75 for our tests. Both high charge ratio and a secondary wick make sure that two nickel wicks can be always replenished with the working fluid.

3. Test results and their analysis

3.1. Characteristic of startup process

Start-up behavior is perhaps considered to be the most complicated transient phenomenon in the LHP operation, the CC filled by liquid can reduce heat leakage from the evaporator and contribute to successful startup. In this test, both the secondary wick and the favorable elevation with a slope of 10° ensure that the wicks were always replenished with liquid. When the shared CC provided two nickel wicks with liquid simultaneously, both heating surface 1 and heating surface 2 might influence mutually, leading to startup failure. However, startup process was quite smooth for this system during the test regardless of heat load applied to one heating surface or two heating surfaces.

3.1.1. Startup process with one heating surface

Startup process with heating surface 2 was investigated at two heat sink temperatures of 0 °C and −5 °C when only one heat source simulator worked. The loop could start up at low heat load of 10 W and the transferred maximum heat load was up to 210 W, corresponding to a heat flux of 21.8 W/cm^2. However, startup process was somewhat different for the same heat load at two heat sink temperatures. Figs. 2 and 3 was the operating temperature curves of 10 W and 30 W at the heat sink temperature of −5 °C.

Fig. 2 was startup process at 10 W applied to heating surface 2 at a heat sink temperature of −5 °C. Based on the temperature change of the condenser inlet, the whole process could be divided into two stages. During the first stage, the temperature of middle vapor line, evaporator ingress and egress rose together owing to back conduction through the evaporator sidewall as soon as heat load was applied to the evaporator wall, subsequently followed by the condenser inlet temperature hopping, the loop seemed to achieve a quasi-steady state. Unfortunately, the condenser inlet temperature only maintained for about 20 min and dropped close to the condenser outlet temperature, implying a failure of the

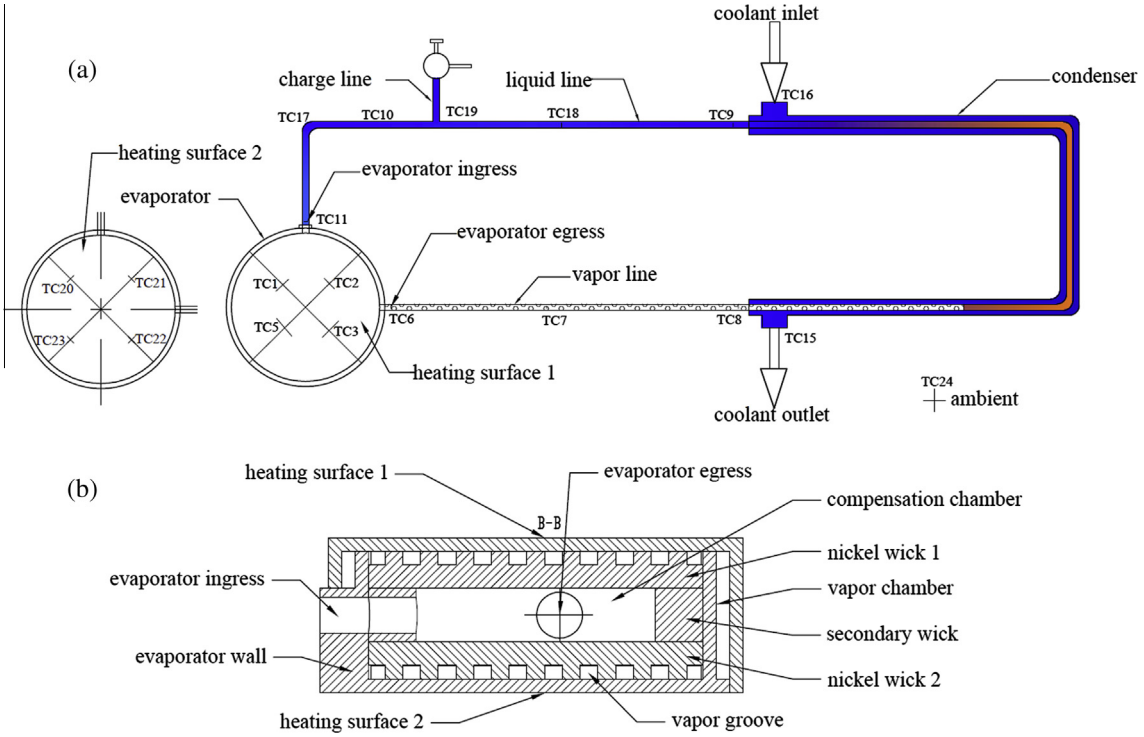

Fig. 1. (a) The schematic diagram of the LHP and locations of the thermocouples; (b) the internal structure of the evaporator.

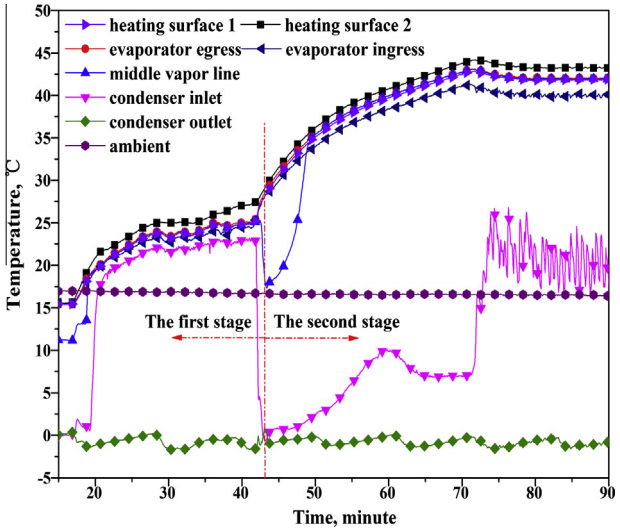

Fig. 2. Startup at 10 W at heat sink temperature of −5 °C.

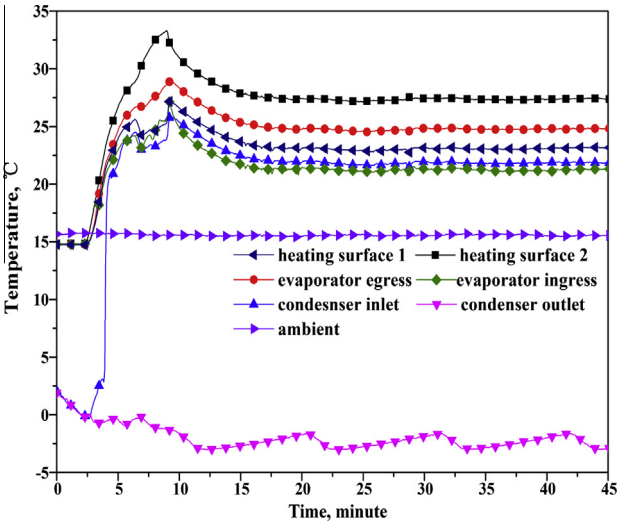

Fig. 3. Startup at 30 W at heat sink temperature of −5 °C.

working fluid circulation. Backward flow of cold liquid from the condenser might result in a decrease of the condenser inlet temperature under the favorable elevation operation. However, the middle vapor line temperature underwent a temperature fluctuation and increased soon, which didn't drop as much as the condenser inlet temperature, indicating that the vapor–liquid interface still existed in the vapor line and just moved out from the condenser. The working fluid circulation restarted when the required pressure difference provided by the temperature difference across the wick was achieved. After a while, the condenser inlet temperature increased stepwise and eventually entered into a temperature fluctuation state, higher than the condenser outlet temperature. Meanwhile, the loop also reached an equilibrium state except for the condenser inlet, this was the second stage. However, startup with 10 W at heat sink temperature of 0 °C described in [23] took less time, about 25 min, to complete the startup process, and had the different working fluid distribution in the condenser.

Fig. 3 showed startup process at 30 W applied to heating surface 2 at a heat sink temperature of −5 °C. The temperature overshoot was noticed obviously, but the loop eventually operated in the steady state and the operating temperature was about 27 °C. The temperature of the evaporator and the condenser inlet almost went up in the meanwhile when 30 W was applied. Along with the process progressing, more cold liquid returned to the CC from the condenser, which could be confirmed by the temperature of the evaporator ingress. The evaporator wall temperature began decreasing, accompanied by the temperature decrease of the condenser inlet. The evaporator wall temperature difference between the highest and the lowest was about 10 °C.

From the view of startup processes with one heating surface, the generated vapor rate was relatively small at low heat load range, the large percentage of the condenser was occupied by the liquid, which decreased the efficiency of the condenser. In addition, small amount of vapor had to overcome the hydrostatic pressure drop caused by the liquid to reach the condenser. Therefore, it was very difficult to keep the stability of the vapor front in the condenser, and the movement of the vapor front directly resulted in the movement of liquid in the condenser [24]. The gravity-assisted condition aggravated the loop operation at low heat load range, and the phenomena of temperature fluctuations and temperature overshoot was easily observed. Decreasing heat sink temperature was unfavorable for startup process at low heat load range, especially for the gravity-assisted operation.

Fig. 4 gave two startup processes with a heat load of 70 W at heat sink temperature of 0 °C and −5 °C. Both of them could start up quickly as soon as heat load was applied, but startup process at heat sink temperature of 0 °C finally operated with temperature fluctuations in synchronism, its frequency and amplitude were 2 min and 4.8 °C, respectively, and startup time was longer. At lower heat sink temperature, startup process showed fast and stable, and the evaporator inlet temperature decreased by 2.3 °C before the system reached the steady state. The vapor was quickly condensed into liquid at lower heat sink temperature of −5 °C. Namely, the ratio of two-phase region to subcooling region will become small. Amount of subcooling carried by the returning liquid at the heat sink temperature of −5 °C was completely compensated for heat leak from the heating zone, which was verified by the temperature decrease of the evaporator ingress. So lower heat sink temperature made the returning liquid more subcooled and reduced the effect of heat leak from the heating zone, which could weaken the fluctuations [25]. Compared with two startup processes under two different conditions, periodic formation and annihilation of bubbles occurred in the CC might be the cause of temperature fluctuations. Lowering heat sink temperature was beneficial to the stabilization of the CC, further contributing to stabilizing the loop at relatively high heat load.

3.1.2. Startup process with the shared CC

In order to confirm the liquid supply of the shared CC to two heating surfaces, startup processes with the shared CC were carried out at heat sink temperature of 0 °C, heat load ranging from 10–10 W to 120–120 W. Namely, the former heat load was loaded to heating surface 1, the later one to heating surface 2. Two heat source simulators attached tightly to heating surface 1 and heating surface 2, respectively. For the evaporator with a shared CC, insufficient liquid supply at high heat load may be a major issue. Thus, 120–120 W were loaded to the evaporator with the operating temperature below (90 ± 2) °C.

Fig. 5 depicted startup characteristics of 120–120 W. According to the figure, startup with 120–120 W demonstrated steady and a fast response to heat load, two heating surfaces possessed similar behavior and the temperature difference between them was less than 1 °C. For operation with one heating surface, the transferred maximum heat load was 210 W with the evaporator wall temperature below (90 ± 2) °C. Therefore, the heat transfer capacity of the evaporator was improved for operation with the shared CC.

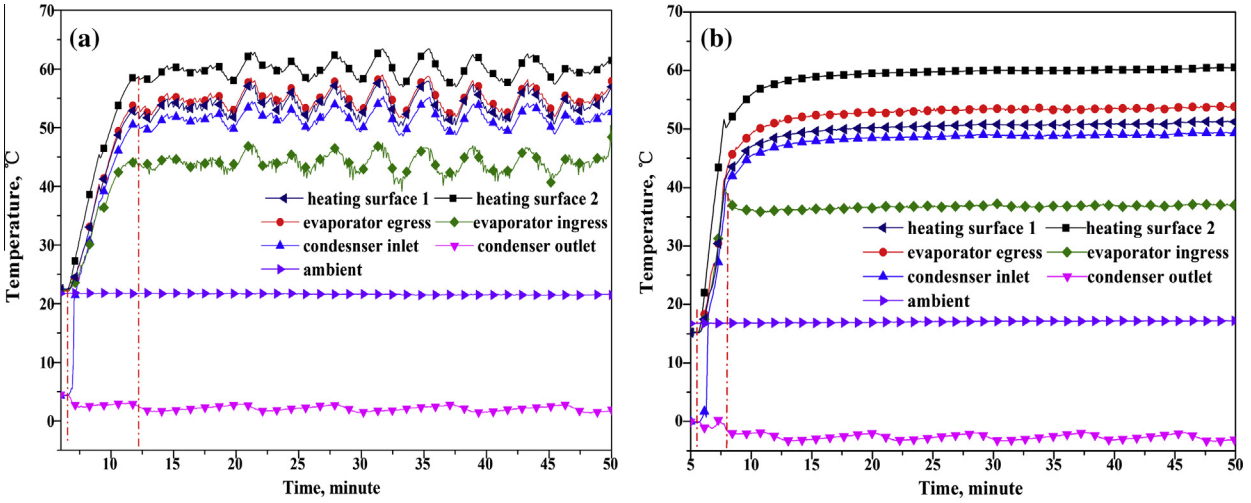

Fig. 4. (a) Startup at 70 W at heat sink temperature of 0 °C; (b) startup at 70 W at heat sink temperature of −5 °C.

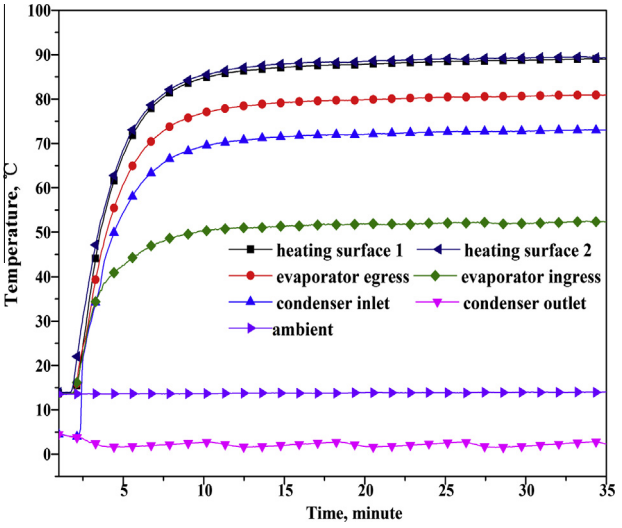

Fig. 5. Startup process at 120–120 W.

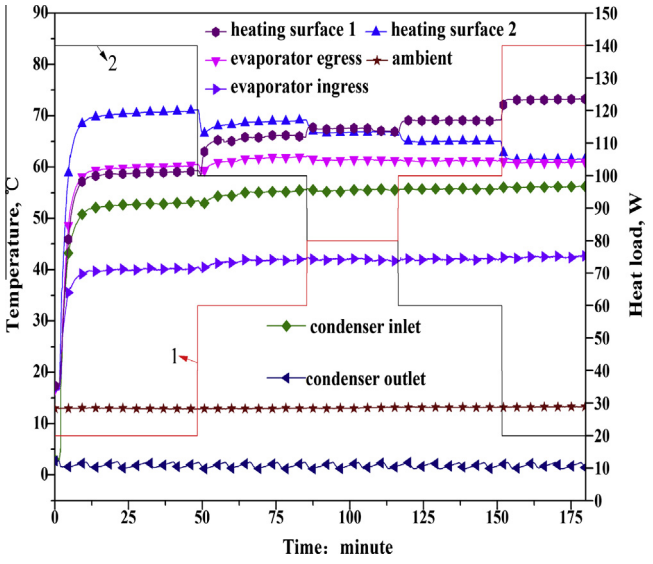

Fig. 6. Continuous operation with alternative heat load.

There existed little difference between startup process with one heating surface and that with the shared CC at high heat load range. For the evaporator with the shared CC, liquid was required supplying to two wicks simultaneously, and startup with equal heat load is an important indicator reflecting the heat transfer performance. Further, good startup performance with the shared CC makes it more beneficial for this system to be applied to cool compact electronics with limited space, such as fuel cells and LED.

3.2. Continuous operation with alternative heat load

The operation under different heat load cycle represents the operational reliability of the LHP. During the tests, continuous operation with the shared CC was examined when heat load was changed in specified way, which similar occasions could be encountered in practical applications. The response of the new evaporator structure to variable heat load demonstrated very fast. Fig. 6 showed the operating curve of two heating surfaces with heat load supplied simultaneously. The evaporator transferred total heat load was fixed at 160 W, each heating surface operated with continuously variable heat load. The way that heat load was arranged was shown in Table 2.

No matter how heat load is applied to two heating surfaces, the heat transfer capacity of the evaporator will maintain a constant value for the fixed total heat load, underlying that the generated rate of vapor, the condenser inlet and outlet temperature, the evaporator ingress and egress temperature also don't change with quantity of heat transfer for each heating surface. For the total heat load of 160 W, the temperature of the condenser inlet and outlet, the evaporator ingress and egress had good isothermality, only the heating surface temperature varied with heat load changing during this test, Fig. 7 described the temperature distribution of two heating surfaces under the same heat load. The maximum temperature difference of 2.6 °C was gained when the value of heat load applied to two heating surfaces was 20 W or 140 W. For heating surface 1, heat load increased stepwise from 20 W to 140 W while decreasing stepwise from 140 W to 20 W for heating surface 2. Vaporization happened on the nickel wick 1 (near heating surface 1) enhanced gradually, more liquid was required reaching the evaporating surface on the nickel wick 1, leading to the increase in flow resistance. Nevertheless, evaporation intensity of the nickel wick 2 receded little by little, accompanied by the decrease in flow resistance. The change of evaporation intensity

Table 2
Heat load arrangement.

Heating surface 1 (W)	20	60	80	100	140
Heating surface 2 (W)	140	100	80	60	20

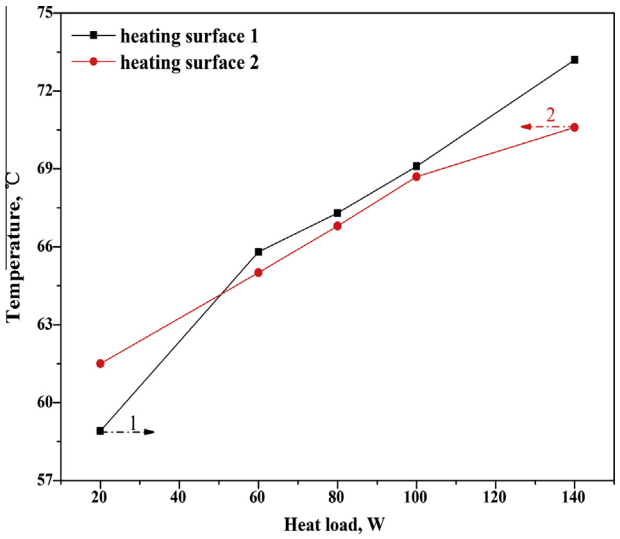

Fig. 7. Temperature variation of two heating surfaces under the same heat load.

resulted in the different distribution of the working fluid inside wicks, and had an influence on the operating temperature. In addition, startup with 20 W for heating surface 1 showed an easy process when heating surface 2 operated at 140 W, which was the result of co-evaporation of two nickel wicks. Because of different vapor–liquid distribution inside two nickel wicks and co-evaporation of two nickel wicks, there existed the temperature difference between two heating surfaces although the same heat load was applied, which distinguished from temperature hysteresis [26]. The temperature of heating surface 1 was higher at operation with the same value of heat load except for 20 W.

3.2. Thermal performance analysis

Thermal resistance from the evaporator to the condenser (R_{LHP}) and thermal resistance of the evaporator (R_{evap}) are usually used to evaluate thermal performance of the LHPs for cooling electronics. R_{LHP} and R_{evap} are respectively defined by the following equations:

$$R_{LHP} = \frac{T_{e2} - T_{cond}}{Q_2} \tag{3}$$

$$R_{evap} = \frac{T_{e2} - T_{e\text{-}out}}{Q_2} = \frac{1}{K_{e0}F_e} \tag{4}$$

and the heat transfer coefficient K_{ei} ($i = 0, 1, 2$; $j = 1, 2$) is regarded as an important indicator of the capacity of the evaporator, and use can be made of the expression:

$$K_{ei} = \frac{Q_j}{F_e(T_{ej} - T_{e\text{-}out})} \tag{5}$$

Fig. 8 showed thermal resistance and the heat transfer coefficient dependence of heat load. The heat transfer coefficient K_{e0} with heating surface 2 only increased at heat load ranging from 10 W to 120 W, and the nucleate boiling occurred on the wick surface [13]. The maximum value K_{e0} of 1.553 W/(cm^2 K) was achieved at 120 W. The vapor film gradually formed on the wick [27] when heat load higher 120 W, inhibiting liquid evaporation.

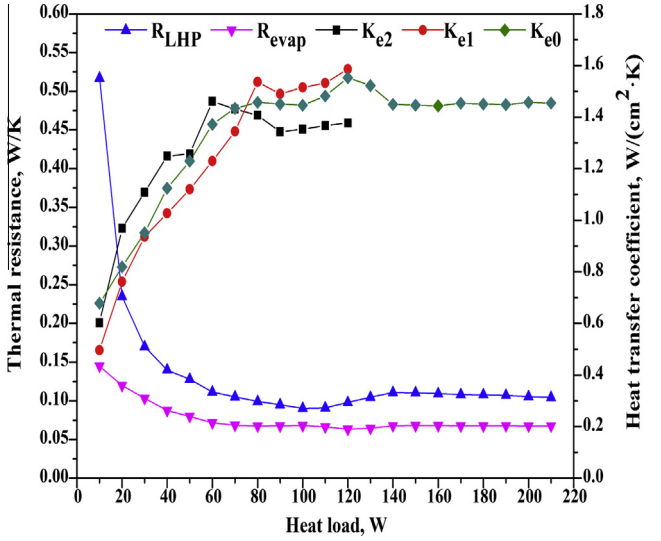

Fig. 8. Analysis of thermal resistance with heating surface 2 at −5 °C and heat transfer coefficient with one surface heated only and two surfaces heated simultaneously.

The value K_{e0} decreased with heat load increasing and eventually maintained at a constant value of 1.454 W/(cm^2 K). Depending on the change of the heat transfer coefficient, two evaporation modes happened on the evaporator wick surface, nucleate boiling and vapor film evaporation. Meanwhile, heat transfer coefficient K_{e1} and K_{e2} were analyzed when equal heat load from 10–10 W to 120–120 W was applied to two surfaces simultaneously. It was found that K_{e0} was always located at between K_{e1} and K_{e2} when heat load smaller than 120 W, and the co-evaporation of two primary wicks had a mutual impact on liquid evaporation.

At low heat loads, the circulation speed of the working fluid was relatively slow, the efficiency of the condenser was comparatively small because of large share of liquid in the condenser. Cold liquid moving along the liquid line gained heat as heat sink temperature was set to be lower than the ambient temperature, smaller amount of subcooling was carried to the CC and heat leak from the evaporator was not sufficiently compensated for, thus leading to higher operating temperature and large total thermal resistance. At heat load between 10 W and 210 W, R_{LHP} ranged from 0.105 K/W to 0.517 K/W. With increment of heat load, Q_2 was mainly transferred to nickel wicks for vaporization, and R_{evap} gradually decreased from 0.145 W/K to 0.068 W/K. Considering that the heating area F_e was a constant value, the heat transfer coefficient K_{e0} from the evaporator wall to the working fluid should increase in principle, indicating that the capacity of heat transfer to the evaporator wall and the wick was improved.

4. Conclusions

An idea, two heating surfaces sharing a compensation chamber, was put forward, and this structure was examined under conditions of the favorable elevation with the slope of 10° (the condenser above the evaporator) and heat sink temperature of 0 °C or −5 °C. Some conclusions could be drawn from the experimental results as follows:

(1) The LHP with a shared CC could start up successfully at heat sink temperatures of 0 °C and −5 °C. At higher heat load, reducing heat sink temperature was beneficial for steady startup, and better performance was achieved at heat sink temperature of −5 °C.

(2) As two heating surfaces were loaded 120–120 W simultaneously, startup process was very successful and smooth, and the temperature difference between two heating surfaces was less than 1 °C.
(3) Under the condition of the constant total heat load of 160 W, the loop demonstrated a fast response to alternative heat load applied to two heating surfaces, and the maximum temperature difference between two heating surfaces was obtained when the value of heat load was 20 W or 140 W.
(4) The co-evaporation of two primary wicks had a mutual impact on operation with two surfaces heated simultaneously.
(5) Heat transfer coefficient for two heating surface 2 was always smaller than one of the two heat transfer coefficients for two surfaces heated simultaneously at heat load less than 120 W.

Conflict of interest

None declared.

Acknowledgement

The current work was supported by the National Natural Science Foundation of China (Grant Nos. 51276071 and 51376069).

References

[1] V.G. Pastukhov, Yu.F. Maidanik, C.V. Vershinin, M.A. Korukov, Miniature loop heat pipes for electronics cooling, Appl. Therm. Eng. 23 (2003) 1125–1135.
[2] Ji Li, Daming Wang, G.P. "Bud" Peterson, A compact loop heat pipe with flat square evaporator for high power chip cooling, IEEE Trans. Compon. Packag. Manu. Technol. 1 (4) (2011) 519–527.
[3] Yu.F. Maydanik, Review: loop heat pipes, Appl. Therm. Eng. 25 (2005) 635–657.
[4] S.C. Wu, D. Wang, J.H. Gao, Z.Y. Huang, Y.M. Chen, Effect of the number of grooves on a wick's surface on the heat transfer performance of loop heat pipe, Appl. Therm. Eng. 71 (2014) 371–377.
[5] G. Kumaresan, S. Venkatachalapathy, Lazarus Godson Asirvatham, Experimental investigation on enhancement in thermal characteristics of sintered wick heat pipe using CuO nanofluids, Int. J. Heat Mass Transfer 72 (2014) 507–516.
[6] Mariya A. Chernysheva, Vladimir G. Pastukhov, Yury F. Maydanik, Analysis of heat exchange in the compensation chamber of a loop heat Pipe, Energy 55 (2013) 253–262.
[7] Tao Fang, Tingzhen Ming, C.P. Tso, Analysis of non-uniform heat loads on evaporators with loop heat pipes, Int. J. Heat Mass Transfer 75 (2014) 313–326.
[8] Yu.F. Maydanik, M.A. Chernysheva, V.G. Pastukhov, Review: loop heat pipes with flat evaporators, Appl. Therm. Eng. 67 (2014) 294–307.
[9] B.B. Chen, W. Liu, Z.C. Liu, H. Li, J.G. Yang, Experimental investigation of loop heat pipe with flat evaporator using biporous wick, Appl. Therm. Eng. 42 (2012) 34–40.
[10] Randeep Singh, Aliakbar Akbarzadeh, Chris Dixon, Masataka Mochizuki, Novel design of a miniature loop heat Pipe evaporator for electronic cooling, J. Heat Transfer 129 (2007) 1445–1452.
[11] Xuan Hung Nguyen, Byung Ho Sung, Jeehoon Choi, Seong Ryoul Ryoo, et al., Study on heat transfer performance for loop heat pipe with circular flat evaporator, Int. J. Heat Mass Transfer 55 (2012) 1304–1315.
[12] Guiping Lin, Nan Li, Lizhan Bai, Dongsheng Wen, Experimental investigation of a dual compensation chamber loop heat pipe, Int. J. Heat Mass Transfer 53 (2010) 3231–3240.
[13] Dongdong Wang, Zhichun Liu, Jun Shen, et al., Experimental study of the loop heat pipe with a flat disk-shaped evaporator, Exp. Thermal Fluid Sci. 57 (2014) 157–164.
[14] Zhichun Liu, Dongdong Wang, Chi Jiang, Jinguo Yang, et al., Experimental study on loop heat pipe with two-wick flat evaporator, Int. J. Thermal Sci. 94 (2015) 9–17.
[15] Chien-Chih Yeh, Chun-Nan Chen, Yau-Ming Chen, Heat transfer analysis of a loop heat pipe with biporous wicks, Int. J. Heat Mass Transfer 52 (2009) 4426–4434.
[16] Huan Li, ZhiChun Liu, BinBin Chen, Wei Liu, Chen Li, Jinguo Yang, Development of biporous wicks for flat-plate loop heat pipe, Exp. Thermal Fluid Sci. 37 (2012) 91–97.
[17] ZhiChun Liu, Huan Li, BinBin Chen, JinGuo Yang, Wei Liu, Operational characteristics of flat type loop heat pipe with biporous wick, Int. J. Thermal Sci. 58 (2012) 180–185.
[18] B.B. Chen, Z.C. Liu, W. Liu, J.G. Yang, H. Li, D.D. Wang, Operational characteristics of two biporous wicks used in loop heat pipe with flat evaporator, Int. J. Heat Mass Transfer 55 (2012) 2204–2207.
[19] Qingjun Cai, Chung-lung Chen, Julie F. Asfia, Multilayer wick structure of loop heat pipe, in: International Mechanical Engineering Congress and Exposition, Seattle, Washington, USA, November 11–15, 2007.
[20] Wei Zhou, Weisong Ling, Lian Duan, K.S. Hui, K.N. Hui, Development and tests of loop heat pipe with multi-layer metal foams as wick structure, Appl. Therm. Eng. 94 (2016) 324–330.
[21] W. Joung, T. Yu, J. Lee, Experimental study on the loop heat pipe with a planar bifacial wick structure, Int. J. Heat Mass Transfer 51 (2008) 1573–1581.
[22] W. Joung, T. Yu, J. Lee, Experimental study on the operating characteristics of a flat bifacial evaporator loop heat pipe, Int. J. Heat Mass Transfer 53 (2010) 276–285.
[23] Dongdong Wang, Zhichun Liu, Song He, Jinguo Yang, et al., Operational characteristics of a loop heat pipe with a flat evaporator and two primary biporous wicks, Int. J. Heat Mass Transfer 89 (2015) 33–41.
[24] Jentung Ku, Low frequency high amplitude temperature oscillations in Loop heat pipe operation, in: 33rd International Conference on Environmental Systems (ICES), Vancouver, B.C., Canada, July 7–10, 2003.
[25] Randeep Singh, Aliakbar Akbarzadeh, Masataka Mochizuki, Operational characteristics of a miniature loop heat pipe with flat evaporator, Int. J. Therm. Sci. 47 (2008) 1504–1515.
[26] Sergey V. Vershinin, Yury F. Maydanik, Hysteresis phenomena in loop heat pipes, Appl. Therm. Eng. 27 (2007) 962–968.
[27] Q. Liao, T.S. Zhao, Evaporative heat transfer in a capillary structure heated by a grooved block, J. Thermophys. Heat Transfer 13 (1999) 126–133.